

Photoproduction of the charged top-pions at the LHeC

Chong-Xing Yue, Jing Guo, Jiao Zhang, Qing-Guo Zeng

Department of Physics, Liaoning Normal University, Dalian 116029, P. R. China *

November 16, 2017

Abstract

The top triangle moose (*TTM*) model, which can be seen as the deconstructed version of the topcolor-assisted technicolor (*TC2*) model, predicts the existence of the charged top-pions π_t^\pm in low energy spectrum. In the context of this model, we consider photoproduction of π_t^\pm via the subprocesses $\gamma b \rightarrow t\pi_t^-$ and $\gamma\bar{b} \rightarrow \bar{t}\pi_t^+$ at the large hadron-electron collider (*LHeC*), in which high energy photon beams are generated by using the Compton backscattering method. We find that, as long as the charged top-pions are not too heavy, they can be abundantly produced via γb collision.

PACS numbers: 12.60.Cn, 14.80.Cp, 13.85.Rm

*E-mail: cxyue@lnnu.edu.cn

1. Introduction

Although the standard model (SM) is an excellent low energy effective theory, the cause of electroweak symmetry breaking ($EWSB$) and the origin of fermion masses continue to be outstanding mystery, which has started to be probed at the LHC . Recently, the $ATLAS$ and CMS collaborations have found some hints of a relatively light Higgs boson with a mass somewhere between 120 and 130 GeV [1]. Thus we are now coming into an exciting period of particle physics.

The top quark is the heaviest elementary particle known up to today. Its mass might has a different origin from the masses of other quarks and leptons, a top quark condensate, $\langle t\bar{t} \rangle$, could be responsible for at least part of $EWSB$. Much theoretical work has been carried out in connection to the top quark and $EWSB$, some specific new physics models are proposed (for review, see [2] and references therein). An interesting model involving a role for the top quark in dynamical $EWSB$ is known as the topcolor-assisted technicolor ($TC2$) model [3]. In the framework of this model, the topcolor, a new QCD – like interaction, that couples strongly to the third generation quarks, makes small contributions to $EWSB$ and gives rise to the main part of the top quark mass. Technicolor (TC) provides the bulk of $EWSB$ via the vacuum expectation value (VEV) of a technifermion bilinear. The light fermions can get masses from the extended technicolor (ETC). The $TC2$ model is one of well-motivated new physics models and has all essential features of the topcolor scenario.

Higgsless models [4] have emerged as a novel way of understanding the mechanism of $EWSB$ without the presence of a scalar particle in the spectrum. Recently, combining Higgsless and topcolor mechanisms, a deconstructed Higgsless model was proposed, called the top triangle moose (TTM) model [5, 6]. In this model, $EWSB$ results largely from the Higgsless mechanism while the top quark mass is mainly generated by the topcolor mechanism. The TTM model alleviates the tension between obtaining the correct top quark mass and keeping $\Delta\rho$ small that exists in many Higgsless models, which can be seen as the deconstructed version of the $TC2$ model.

The new physics models belonging to the topcolor scenario genetically have two sources of $EWSB$ and there are two sets of Goldstone bosons. One set is eaten by the electroweak gauge bosons W and Z to generate their masses, while the other set remains in the spectrum, which is called the top-pions (π_t^0 and π_t^\pm). Topcolor scenario also predicts the existence of the top-Higgs h_t^0 , which is the $t\bar{t}$ bound state. It is well known that the possible signals of these new scalar particles have been extensively studied in the literature. However, most of works are done in the context of the $TC2$ model.

More phenomenology analysis about the top-pions and top-Higgs predicted by the TTM model is needed. Although photoproduction of the charged top-pions has been studied in Ref.[7], which proceeds via the subprocess $\gamma c \rightarrow b\pi_t^+$ mediated by the flavor changing couplings. The high energy photon beams are generated by using the Compton backscattering of the initial electron and laser photon beams. However, so far, photoproduction of the charged top-pions via the subprocesses $\gamma b \rightarrow t\pi_t^-$ and $\gamma\bar{b} \rightarrow \bar{t}\pi_t^+$ has not been considered at the large hadron-electron collider ($LHeC$). Furthermore, many popular models beyond the SM predict the existence of the charged scalars. At the $LHeC$, these new particles can be produced via γb collision, which has not been detailed studied in the literature, as we know. Thus, in this paper, we will consider photoproduction of the charged top-pion associated with a top quark in the frameworks of the TTM and $TC2$ models and compare the numerical results with each other. Our calculation can be easily transformed to other models. We hope that our works will be helpful to test topcolor models and further to distinguish different new physics models at the $LHeC$.

The layout of the present paper is as follows. After reviewing the essential features of the TTM model in section 2, we calculate the production cross section of the subprocess $\gamma b \rightarrow t\pi_t^-$ at the $LHeC$ in section 3. To compare our numerical results with those of the $TC2$ model, we further consider photoproduction of the charged top-pions predicted by the $TC2$ model in section 4. Our conclusion and discussion are given in section 5.

2. The essential features of the TTM model

The detailed description of the TTM model can be found in Refs.[5, 6], and here we just want to briefly review its essential features, which are related to our calculation.

The electroweak gauge structure of the TTM model is $SU(2)_0 \times SU(2)_1 \times U(1)_2$. The nonlinear sigma field Σ_{01} breaks the group $SU(2)_0 \times SU(2)_1$ down to $SU(2)$ and field Σ_{12} breaks $SU(2)_1 \times U(1)_2$ down to $U(1)$. To separate top quark mass generation from $EWSB$, a top-Higgs field Φ is introduced to the TTM model, which couples preferentially to the top quark. To ensure that most of the $EWSB$ comes from the Higgsless side, the $VEVs$ of the fields Σ_{01} and Σ_{12} are chosen to be $\langle \Sigma_{01} \rangle = \langle \Sigma_{12} \rangle = F = \sqrt{2}\nu \cos \omega$, in which $\nu = 246 GeV$ is the electroweak scale and ω is a new small parameter. The VEV of the top-Higgs field is $f = \langle \Phi \rangle = \nu \sin \omega$.

From above discussions, we can see that, for the TTM model, there are six scalar degrees of freedom on the Higgsless sector and four on the top-Higgs sector. Six of these Goldstone bosons are eaten to give masses to the gauge bosons W^\pm , Z , W'^\pm and Z' . Others remain as physical states in the spectrum, which are called the top-pions (π_t^\pm and π_t^0) and the top-Higgs h_t^0 . In this paper, we will focus our attention on photoproduction of the charged top-pions at the $LHeC$. The couplings of the charged top-pions π_t^\pm to ordinary particles, which are related our calculation, are given by [6]

$$\mathcal{L}_{\pi_t tb} = i\lambda_t \cos \omega \left\{ 1 - \frac{x^2[a^4 + (a^4 - 2a^2 + 2) \cos 2\omega]}{8(a^2 - 1)^2} \right\} (\pi_t^+ \bar{t} b P_L + \pi_t^- \bar{t} b P_R) \quad (1)$$

with

$$\lambda_t = \frac{\sqrt{2}m_t}{\nu \sin \omega} \left[\frac{M_D^2(\varepsilon_L^2 + 1) - m_t^2}{M_D^2 - m_t^2} \right], \quad a = \frac{\nu \sin \omega}{\sqrt{2}M_D}, \quad x = \sqrt{2}\varepsilon_L = \frac{2 \cos \omega M_W}{M_{W'}}. \quad (2)$$

Here $P_{L(R)} = \frac{1}{2}(1 \mp \gamma_5)$ is the left(right)-handed projection operator, M_D is the mass scale of the heavy fermion and $M_{W'}$ is the mass of the new gauge boson W' . Since the top quark mass depends very little on the right-handed delocalization parameter ε_{tR} , we have set $\varepsilon_{tR} = 0$ in $Eq.(1)$. The parameter ε_L describes the degree of delocalization of the left-handed fermions and is flavor universal, the parameter x presents the ratio of gauge couplings. The relationship between ε_L and x , which is given in $Eq.(2)$, is imposed by ideal delocalization.

Reference [8] has shown that $M_{W'}$ should be larger than 380GeV demanded by the $LEP\text{II}$ data and smaller than 1.2TeV by the need to maintain perturbative unitarity in $W_L W_L$ scattering. It is obvious that the coupling $\pi_t t b$ is not very sensitive to the parameters $M_{W'}$ and M_D . Thus, the production cross sections of the subprocesses $\gamma b \rightarrow t \pi_t^-$ and $\gamma \bar{b} \rightarrow \bar{t} \pi_t^+$ are not strongly dependent on the values of the mass parameters $M_{W'}$ and M_D . In our following numerical calculation, we will take the illustrative values $M_{W'} = 500\text{GeV}$ and $M_D = 650\text{GeV}$. In this case, there is $[M_D^2(\varepsilon_L^2 + 1) - m_t^2]/(M_D^2 - m_t^2) \approx 1$ and Eq.(1) can be approximately written as

$$\mathcal{L}_{\pi_t t b} \approx i \frac{\sqrt{2} m_t C}{\nu} \cot \omega (\pi_t^+ \bar{t} b P_L + \pi_t^- t \bar{b} P_R) \quad (3)$$

with

$$C = 1 - \frac{x^2 [a^4 + (a^4 - 2a^2 + 2) \cos 2\omega]}{8(a^2 - 1)^2}. \quad (4)$$

It is obvious that constant C is not sensitive to the value of $\sin \omega$ and its value close to 1.

3. Photoproduction of the charged top-pions at the $LHeC$ within the TTM model

Recently, the high-energy ep collision has been considered at the LHC , which is called the $LHeC$ [9, 10]. At the $LHeC$, the incoming proton beam has an energy $E_p = 7\text{TeV}$ and the energy E_e of the incoming electron is in the range of $50 \sim 200\text{GeV}$, corresponding to the center-of-mass ($c.m.$) energy of $\sqrt{s} = 2\sqrt{E_p E_e} \approx 1.18 \sim 2.37\text{TeV}$. Its anticipated integrated luminosity is at the order of $10 \sim 100\text{fb}^{-1}$ depending on the energy of the incoming electron and the design. The $LHeC$ can be used to accurately determine the parton dynamics and the momentum distributions of quarks and gluons in proton. Furthermore, it can provide better condition for studying a lot of phenomena comparing to the high energy linear e^+e^- collider (ILC) due to the high $c.m.$ energy and to the LHC due to more clear environment [10, 11]. Thus, it may play a significant role in the discovery of new physics beyond the SM . An other advantage of the $LHeC$ is the opportunity to construct γp collider [12] with the photon beam generated by the backward

Compton scattering of incident electron- and laser-beams. The energy and luminosity of the photon beam would be the same order of magnitude of the parent electron beam.

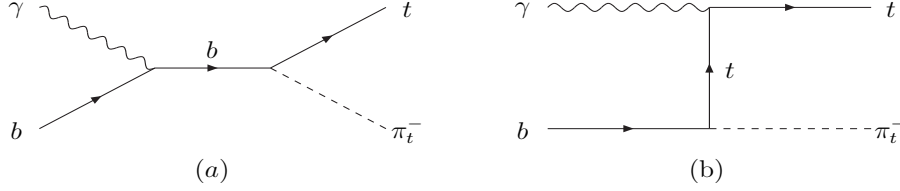


Figure 1: Feynman diagrams for the subprocess $\gamma b \rightarrow t\pi_t^-$.

From the discussions given in section 2, we can see that the charged top-pion π_t^- can be produced via the subprocess $\gamma(k_1)b(p_1) \rightarrow t(p_2)\pi_t^-(k_2)$ at the *LHeC*. The relevant Feynman diagrams are depicted in *Fig.1*. With the relevant couplings, the invariant production amplitude can be written as

$$\begin{aligned}
M &= M_a + M_b \\
&= A \bar{u}(p_2) P_R \frac{i}{\not{k}_1 + \not{p}_1} \left(-\frac{1}{3}e\gamma^\mu\right) u(p_1) \varepsilon_\mu(k_1) \\
&\quad + A \bar{u}(p_2) \left(\frac{2}{3}e\gamma^\mu\right) \frac{i}{\not{p}_2 - \not{k}_1 - m_t} P_R u(p_1) \varepsilon_\mu(k_1)
\end{aligned} \tag{5}$$

with

$$A = \frac{\sqrt{2}m_t C}{\nu} \cot \omega. \tag{6}$$

Here $\varepsilon_\mu(k_1)$ is the polarization vector of the photon. In above equation, we have taken $m_b \approx 0$. Using the amplitude M , we can directly obtain the cross section $\hat{\sigma}(\hat{s})$ for the subprocess $\gamma b \rightarrow t\pi_t^-$.

Since the photon beam in γb collision is generated by the Compton backscattering of the incident electron- and the laser-beams, the effective cross section $\sigma_1(s)$ at the *LHeC* can be obtained by folding $\hat{\sigma}(\hat{s})$ with the bottom quark and photon distribution functions. For this purpose, we define the variables: $\hat{s} = x_1 x_2 s$ with $x_1 = E_\gamma/E_e$ and $x_2 = E_b/E_p$. \sqrt{s} is the *c.m.* energy of the *LHeC*. The cross section $\sigma_1(s)$ for the process

$ep \rightarrow \gamma b + X \rightarrow t\pi_t^- + X$ can be given by

$$\sigma_1(s) = \int_{(m_{\pi_t} + m_t)^2/s}^{x_{1max}} dx_1 \int_{(m_{\pi_t} + m_t)^2/x_1 s}^1 dx_2 f_{\gamma/e}(x_1) f_{b/p}(x_2) \hat{\sigma}(\hat{s}). \quad (7)$$

For unpolarized initial electron and laser beams, the energy spectrum of the backscattered photon is [13]

$$f_{\gamma/e}(x) = \frac{1}{D(\xi)} \left\{ 1 - x + \frac{1}{1-x} \left[1 - \frac{4x}{\xi} \left(1 - \frac{x}{\xi(1-x)} \right) \right] \right\} \quad (8)$$

with

$$D(\xi) = \left(1 - \frac{4}{\xi} - \frac{8}{\xi^2} \right) \ln(1 + \xi) + \frac{1}{2} + \frac{8}{\xi} - \frac{1}{2(1 + \xi)^2}. \quad (9)$$

Where $\xi = 4E_e E_0 / m_e^2$ in which m_e denotes the incident electron mass, E_0 denotes the initial laser photon energy. x is the fraction of energy taken by the backscattered photon beam moving along the initial electron direction. $f_{\gamma/e}(x)$ vanishes for $x > x_{max} = E_{max}/E_e = \xi/(1 + \xi)$. In order to get ride of the background effects in the Compton backscattering, particularly e^+e^- pair production in the collision of the laser with the backscattered photon, it is required $E_0 x_{max} \leq m_e^2/E_e$ which implies $\xi \leq 2 + 2\sqrt{2} \approx 4.83$ [13]. For the choice $\xi = 4.8$, one can obtain $x_{max} \approx 0.83$ and $D(\xi) \approx 1.84$. In *Eq.(7)*, the bottom quark is directly taken from the proton in a five flavor scheme. For the bottom quark distribution function $f_{b/p}(x_2)$, we will use the form given by the *CTEQ6L* [14] parton distribution functions (*PDFs*). The renormalization and factorization scales are taken as the $t\pi_t^-$ invariant mass.

Except for the *SM* input parameters $\alpha_e = 1/128$, $m_t = 172 GeV$, and $M_W = 80.4 GeV$ [14], the production cross section for the process $ep \rightarrow t\pi_t^- + X$ is dependent on the free parameters $\sin \omega$ and m_{π_t} . The parameter $\sin \omega$ indicates the fraction of *EW SB* provided by the top condensate. The top-pion mass m_{π_t} depend on the amount of top-quark mass arising from the *ETC* sector and on the effects of electroweak gauge interactions [2], and thus its value is model-dependent. In the context of the *TTM* model, Ref.[6] has obtained the constraints on the top-pion mass via studying its effects on the relevant experimental observables. Similarly with Refs.[6, 16], we will assume that the values of

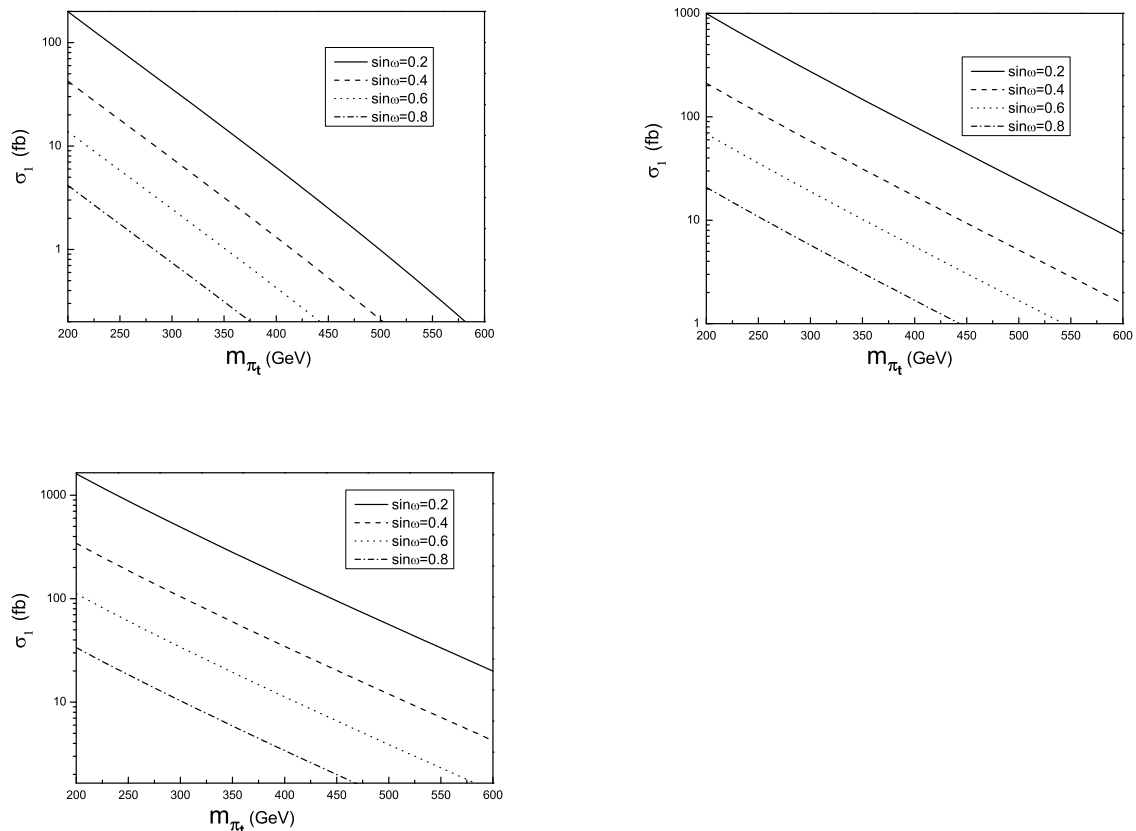


Figure 2: The cross section $\sigma_1(s)$ as a function of the mass parameter m_{π_t} for $E_e = 70\text{GeV}$ (a), 150GeV (b) and 200GeV (c).

the free parameters $\sin\omega$ and m_{π_t} are in the ranges of $0.2 \sim 0.8$ and $200 \sim 600\text{GeV}$, respectively.

Our numerical results are summarized in *Fig.2*, in which we have plotted the production cross section $\sigma_1(s)$ as a function of the charged top-pion mass m_{π_t} for $E_e = 70\text{GeV}$, 150GeV and 200GeV , and various values of the parameter $\sin\omega$. One can see that, for $70\text{GeV} \leq E_e \leq 200\text{GeV}$, $200\text{GeV} \leq m_{\pi_t} \leq 600\text{GeV}$, and $0.2 \leq \sin\omega \leq 0.8$, the value of the cross section $\sigma_1(s)$ for the process $ep \rightarrow t\pi_t^- + X$ is in the range of $2.8 \times 10^{-3}fb \sim 1.6 \times 10^3fb$, which is sensitive to the free parameters $\sin\omega$ and m_{π_t} . If we assume that the yearly integrated luminosity $\mathcal{L}_{Lint} = 50fb^{-1}$, than there will be several

and up to ten thousands of $t\pi_t^-$ events to be generated at the $LHeC$ per year.

It is well known that, for a heavy charged scalar, which is heavier than the top quark, the main production channel proceeds via gluon-bottom collision at the LHC . In the context of the TTM model, Ref.[6] has studied production of the charged top-pion π_t^- via the subprocess $gb \rightarrow t\pi_t^-$ and discussed the possibility of detecting the charged top-pions at the LHC . It is obvious that the $t\pi_t^-$ production cross section at the LHC with $\sqrt{s} = 14TeV$ is larger than that at the $LHeC$ with $\sqrt{s} = 2.37TeV$ as shown in Fig.2. However, considering the more clear environment comparing to the LHC , it is needed to consider the subprocess $\gamma b \rightarrow t\pi_t^-$ in the near future $LHeC$ experiments.

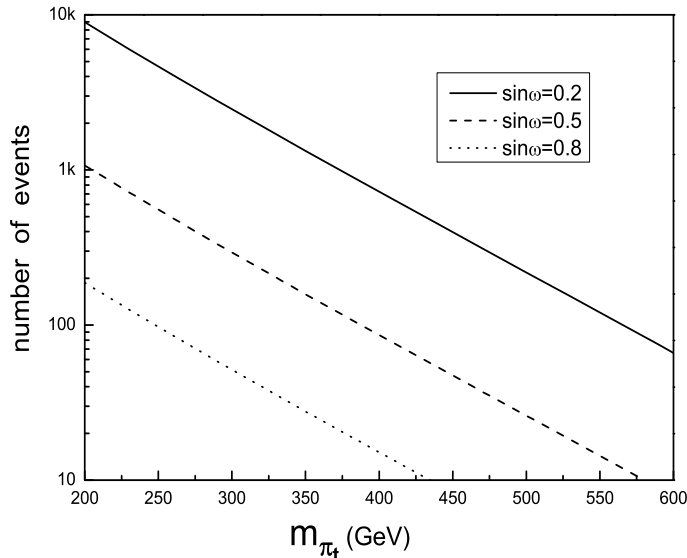


Figure 3: The number of the $l^+l^- + bbb + \cancel{E}$ signal events generated at the $LHeC$.

Reference [6] has shown that, for $m_{h_t} \geq 300GeV$ and $m_{\pi_t} \leq 600GeV$, the charged top-pions π_t^\pm dominantly decay into tb and there is $Br(\pi_t^\pm \rightarrow tb) > 90\%$. Thus, photoproduction of the charged top-pion associated a top quark can easily transfer to the $t\bar{t}b$ final state. In order to ensure the clearest event signature, only fully leptonic decay modes of the gauge boson W are considered. Then, photoproduction of the charged top-pions can give rise to the $l^+l^- + bbb + \cancel{E}$ signature at the $LHeC$. Its production rate can be easily

estimated by multiplying the overall decay branching ratios to the effective production cross section, which can be approximately written as: $[\sigma_1(t\pi_t^-) + \sigma_1(\bar{t}\pi_t^+)] \times [Br(t \rightarrow Wb)]^2 \times Br(\pi_t^\pm \rightarrow tb) \times [Br(W \rightarrow l\nu)]^2 \approx 2\sigma_1 \times 1 \times 0.9 \times (3 \times 0.108)^2 \approx 0.18\sigma_1$. In this estimation, we have assumed that the production cross section of the subprocess $\gamma\bar{b} \rightarrow \bar{t}\pi_t^+$ equals to that for the subprocess $\gamma b \rightarrow t\pi_t^-$, and taken $Br(t \rightarrow Wb) \approx 1$ and $Br(W^\pm \rightarrow e\nu_e) \simeq Br(W^\pm \rightarrow \mu\nu_\mu) \simeq Br(W^\pm \rightarrow \tau\nu_\tau) \simeq 10.8\%$. The number of the signal events generated at the *LHeC* per year are given in *Fig.3*, in which we have taken $E_e = 150\text{GeV}$ and the yearly integrated luminosity $\mathcal{L}_{Lint} = 50\text{fb}^{-1}$. One can see from this figure that, in wide range of the parameter space of the *TTM* model, there will be thousands of the $l^+l^- + bbb + \cancel{E}$ signal events to be generated at the *LHeC*. If the electroweak gauge boson W decays to $l\nu$ with l denoting e or μ , the number of the signal events will be reduced. However, this allows the invariant mass of the charged top-pion to be reconstructed, which help separate the signal from the large $t\bar{t} + jets$ background. Certainly, detailed confirmation of the observability of the signals generated by the process $ep \rightarrow t\pi_t^\pm + X$, would require Monte Carlo simulation of the signals and the relevant *SM* backgrounds, which is beyond the scope of this paper.

4. Photoproduction of the charged top-pions at the *LHeC* within the *TC2* model

To solve the phenomenological difficulties of traditional *TC* theory, topcolor models [2] were proposed by combining *TC* interactions with the topcolor interactions at the scale of about 1TeV . It is well known that the *TC2* model [3] is one of the phenomenologically viable models, which has almost all essential features of this kind of new physics models.

For the *TC2* model [3], *TC* interaction plays the main role in *EWSB*. Topcolor interaction makes small contributions to *EWSB* and gives rise to the main part of the top quark mass, $(1 - \varepsilon)m_t$, with the parameter $\varepsilon \ll 1$. Thus, there is the relation

$$\nu_\pi^2 + F_t^2 = \nu_W^2. \quad (10)$$

Where ν_π represents the contributions of *TC* interactions to *EWSB*, $\nu_W = \nu/\sqrt{2} =$

174GeV. Here F_t is the physical top-pion decay constant, which can be estimated from the Pagels-Stokar formula and written as

$$F_t^2 = \frac{N_c}{16\pi^2} m_{t,dyn}^2 \ln\left(\frac{\Lambda^2}{m_{t,dyn}^2}\right). \quad (11)$$

Where $N_c = 3$ is the color factor, Λ is the cutoff scale and $m_{t,dyn}$ denotes the portion of the top quark mass generated by the topcolor interaction. In the case of $m_{t,dyn} \approx m_t$ and $1TeV \leq \Lambda \leq 20TeV$, Ref.[16] has shown that the value of the factor $\sin\omega = F_t/\nu_W$ is in the range of 0.25 and 0.5. Allowing F_t to vary over this ranges does not qualitatively change our conclusion, thus, we will take $F_t = 50GeV$ for illustration in our numerical analysis, which corresponds to $\Lambda = 1.59TeV$.

In the *TC2* model, topcolor interaction is not flavor-universal and mainly couples to the third generation quarks. Thus, the top-pions (π_t^\pm, π_t^0) have large Yukawa couplings to the third family. The explicit forms for the couplings of π_t^\pm to the third generation quarks, which are related our calculation, can be written as [3, 17]

$$\frac{(1-\varepsilon)m_t}{F_t} \frac{\sqrt{\nu_w^2 - F_t^2}}{\nu_w} (\pi_t^+ \bar{t}b P_L + \pi_t^- \bar{t}b P_R). \quad (12)$$

Where the factor $\sqrt{\nu_w^2 - F_t^2}/\nu_w$ reflects the effects of the mixing between the top-pion and the electroweak Goldstone boson of the *TC* sector.

It is obvious that the charged top-pions π_t^\pm predicted the *TC2* model can also be produced via the subprocesses $\gamma b \rightarrow t\pi_t^-$ and $\gamma \bar{b} \rightarrow \bar{t}\pi_t^+$ at the *LHeC*. The effective production cross section σ_2 only depends on two free parameters ε and m_{π_t} . The parameter ε parameterizes the portion of the *ETC* contributions to the top quark mass. From theoretical point of view, ε with value from 0.01 to 0.1 is favored. The cross section σ_2 depends on the free parameter ε only via the factor $(1-\varepsilon)^2$, thus its value is not sensitive to the free parameter ε and we will take $\varepsilon = 0.05$ in our numerical estimation. For the top-pion mass, the mass splitting between the neutral top-pion and the charged top-pion is very small, since it comes only from the electroweak interactions [18]. The absence of $t \rightarrow \pi_t^+ b$ implies that $m_{\pi_t^+} > 165GeV$ [19] and the branch ratio R_b for the decay $Z \rightarrow b\bar{b}$

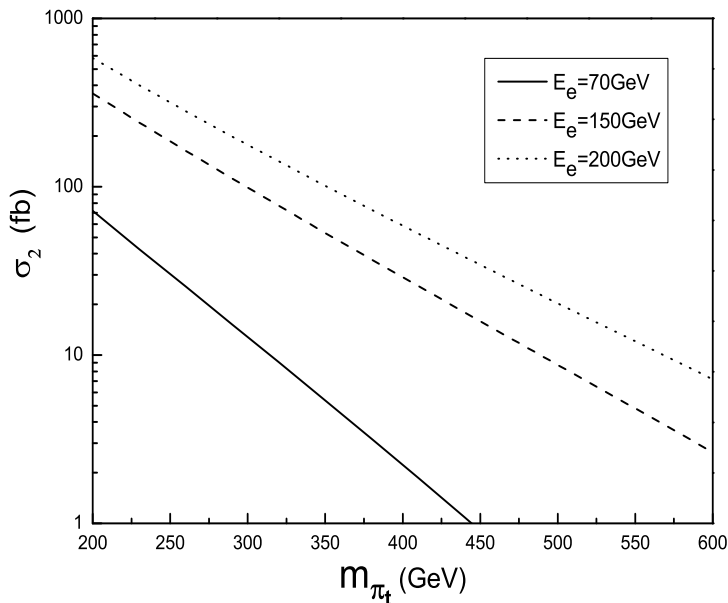


Figure 4: The cross section $\sigma_2(s)$ as a function of the mass parameter m_{π_t} for $E_e = 70\text{GeV}$, 150GeV and 200GeV .

yields $m_{\pi_t^+} > 220\text{GeV}$ [20]. In this paper, we will take $m_{\pi_t^0} = m_{\pi_t^\pm} = m_{\pi_t}$ and assume that its value is in the range of $200 \sim 600\text{GeV}$.

The production cross section σ_2 for the process $ep \rightarrow t\pi_t^- + X$ is plotted in *Fig.4* as a function of the mass parameter m_{π_t} for the parameters $\varepsilon = 0.05$ and $E_e = 70\text{GeV}$, 150GeV , 200GeV . One can see from this figure that the cross section is larger than that for the *TTM* model with $\sin\omega \geq 0.3$. For $\varepsilon = 0.05$, $200\text{GeV} \leq m_{\pi_t} \leq 600\text{GeV}$, and $70\text{GeV} \leq E_e \leq 200\text{GeV}$, the value of the cross section σ_2 is in the range of $5 \times 10^{-2} \sim 5.8 \times 10^2\text{fb}$.

Reference [21] has shown that, in most of the parameter space of the *TC2* model, the charged top-pions π_t^\pm mainly decay to the modes tb and cb with the branching ratio about 70% and 30%, respectively. For the decay mode tb , photoproduction of the charged top-pions at the *LHeC* would give rise to the $t\bar{t}b$ final state, which is same as that in the *TTM* model. For the decay channel $\pi_t^\pm \rightarrow bc$ induced by the flavor changing interactions

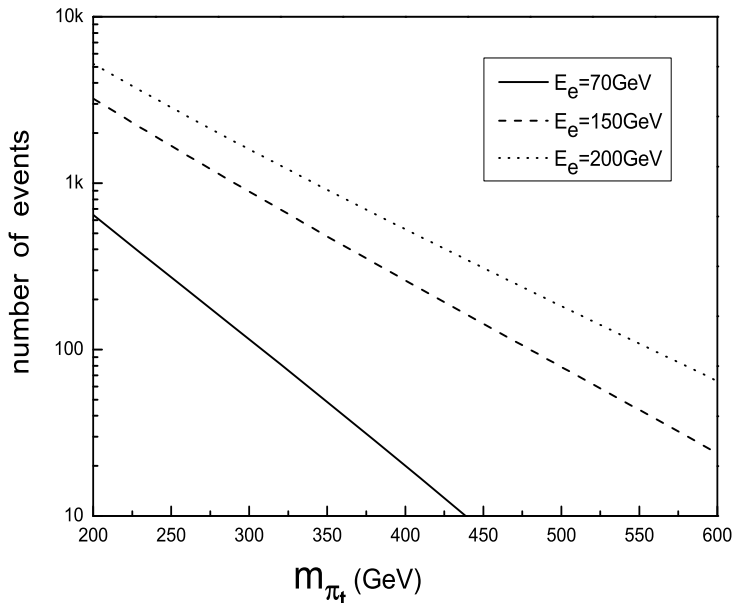


Figure 5: The number of the $l^\pm + bb + jet + \cancel{E}$ events generated at the $LHeC$.

[17], it would give rise to the $tb\bar{c}$ final state, which induces the $l^\pm + bb + jet + \cancel{E}$ and $bb + 3jets$ signature for W^\pm leptonic decay, $W^\pm \rightarrow l\nu$ and W^\pm hadronic decay, $W^\pm \rightarrow qq'$, respectively. The number of the $l^\pm + bb + jet + \cancel{E}$ events are shown in *Fig.5* as a function of the mass parameter m_{π_t} for $E_e = 150\text{GeV}$. one can see from this figure that, for $200\text{GeV} \leq m_{\pi_t} \leq 500\text{GeV}$, there will be $78 \sim 3226$ $l^\pm + bb + jet + \cancel{E}$ events to be generated per year at the $LHeC$ with $\mathcal{L}_{Lint} = 50\text{fb}^{-1}$.

5. Conclusion and discussion

A common feature of the new physics model belonging to the topcolor scenario is the prediction of the charged top-pions in the low energy spectrum, regardless of the dynamics responsible for $EWSB$ and light quark masses. It is well known that, for the heavy charged scalar, which is heavier than the top quark, the subprocesses $gb \rightarrow tS^-$ and $g\bar{b} \rightarrow \bar{t}S^+$ are one kind of important production channels at the LHC . At the $LHeC$, the charged scalars can be produced via γb collision, which has not been detailed studied

in the literature, as we know. In this paper, we consider photoproduction of the charged top-pions predicted by the *TTM* and *TC2* models, which proceed via the subprocesses $\gamma b \rightarrow t\pi_t^-$ and $\gamma \bar{b} \rightarrow \bar{t}\pi_t^+$ at the *LHeC*.

Our numerical results show that, in the frameworks of both the *TTM* model and the *TC2* model, the charged top-pions π_t^\pm can be abundantly produced via γb collision, as long as they are not too heavy. In the *TC2* model, the production cross section is only sensitive to the model-dependent parameter m_{π_t} , while it is sensitive to the free parameters $\sin\omega$ and m_{π_t} in the *TTM* model. For $\sin\omega < 0.3$, the cross section of the process $ep \rightarrow t\pi_t^- + X$ is larger than that in the *TC2* model. For example, for $\sin\omega = 0.2$, $E_e = 150\text{GeV}$ and $200\text{GeV} \leq m_{\pi_t} \leq 600\text{GeV}$, the value of $\sigma_1(t\pi_t^-)$ for the process $ep \rightarrow t\pi_t^- + X$ is in the range of $7.3 \sim 995\text{fb}$, while its value is in the range of $5 \times 10^{-2} \sim 5.8 \times 10^2\text{fb}$ in most of the parameter space of the *TC2* model.

The minimal supersymmetric standard model (*MSSM*) [22] also predicts the existence of the charged scalars, which can also be produced via the subprocesses $\gamma b \rightarrow tS^-$ and $\gamma \bar{b} \rightarrow \bar{t}S^+$ at the *LHeC*. For the type II two-Higgs doublet models (*2HDMs*) [23], the tree-level production cross sections are proportional to $(m_t^2 \cot^2 \beta + m_b^2 \tan^2 \beta)$, while proportional to $\cot^2 \beta$ for the type I *2HDMs*. Thus, photoproduction cross sections of the charged scalars predicted by the *MSSM* are larger or smaller than those of the *TTM* model or the *TC2* model, which depend on the parameter $\tan\beta$.

Acknowledgments

This work was supported in part by the National Natural Science Foundation of China under Grants No.10975067, the Specialized Research Fund for the Doctoral Program of Higher Education (SRFDP) (No.200801650002), the Natural Science Foundation of the Liaoning Scientific Committee (No. 201102114), and Foundation of Liaoning Educational Committee (No. LT2011015).

References

- [1] ATLAS collaboration, arXiv:1202.1408 [hep-ex]; arXiv:1202.1414 [hep-ex]; CMS collaboration, arXiv:1202.1416 [hep-ex]; arXiv:1202.1487 [hep-ex]; arXiv:1202.1488 [hep-ex]; arXiv:1202.1489 [hep-ex].
- [2] G. Cvetič, *Rev. Mod. Phys.* **71**, 513(1999); C. T. Hill and E. H. Simmons, *Phys. Rept.* **381**, 235(2003); [Erratum-ibid, **390**, 553(2004)].
- [3] C. T. Hill, *Phys. Lett. B* **345**, 483(1995); K. D. Lane and E. Eichten, *Phys. Lett. B* **352**, 382(1995); K. D. Lane, *Phys. Lett. B* **433**, 96(1998).
- [4] C. Csaki, C. Grojean, H. Murayama, L. Pilo, J. Terning, *Phys. Rev. D* **69**, 055006(2004).
- [5] R. S. Chivukula, N. D. Christensen, B. Coleppa, and E. H. Simmons, *Phys. Rev. D* **80**, 035011(2009).
- [6] R. S. Chivukula, E. H. Simmons, B. Coleppa, H. E. Logan, A. Martin, *Phys. Rev. D* **83**, 055013(2011).
- [7] Chong-Xing Yue, Hong-Jie Zong, Shun-Zhi Wang, *Phys. Lett. B* **575**, 25(2003); Guo-Li Liu, *Phys. Rev. D* **82**, 115032(2010).
- [8] R. S. Chivukula *et al*, *Phys. Rev. D* **74**, 075011(2006) .
- [9] The LHeC web page, <http://www.lhec.org.uk>.
- [10] J. B. Dainton, M. Klein, P. Newman, E. Perez, and F. Willeke, *JINST* **1**, P10001(2006); P. Newman, *Nucl. Phys. Proc. Suppl.* **191**, 307(2009); A. N. Akay, H. Karadeniz, S. Sultansoy, *Int. J. Mod. Phys. A* **25**, 4589(2010).
- [11] S. Sultansay, *Eur. Phys. J. C* **33**, S1064(2004), and references therein.

- [12] S. I. Alekhin et al., *Int. J. Mod. Phys. A* **6**, 21(1991); A. K. Ciftci et al., *Nucl. Instrum. Meth. A* **365**, 317(1995); A. K. Ciftci, S. Sultansoy, O. Yavas, *Nucl. Instrum. Meth. A* **472**, 72(2001); H. Aksakal et al., *Nucl. Instrum. Meth. A* **576**, 287(2007).
- [13] I. F. Ginzburg, G. L. Kotkin, V. G. Serbo, V. I. Telnov, *Nucl. Instrum. Meth.* **205**, 47(1983); I. F. Ginzburg, et al., *Nucl. Instrum. Meth., A* **219**, 5(1984); V. I. Telnov, *Nucl. Instrum. Meth., A* **294**, 72(1990).
- [14] J. Pumplin et al. (CTEQ Collaboration), *JHEP* **0602**, 032(2006).
- [15] K. Nakamura et al. [Particle Data Group], *J. Phys. G* **37**, 075021(2010).
- [16] R. S. Chivukula et al., *Phys. Rev. D* **84**, 095022(2011).
- [17] G. Burdman, *Phys. Rev. Lett.* **83**, 2888(1999); H.-J. He, C.-P. Yuan, *Phys. Rev. Lett.* **83**, 28(1999); H.-J. He, S. Kanemura, C.-P. Yuan, *Phys. Rev. Lett.* **89**, 101803(2002).
- [18] C. T. Hill, *Phys. Lett. B* **266**, 419(1991).
- [19] B. Balaji, *Phys. Lett. B* **393**, 89(1997).
- [20] G. Burdman and D. Kominis, *Phys. Lett. B* **403**, 101(1997); W. Loinaz and T. Takeuchi, *Phys. Rev. D* **60**, 015005(1999); C. T. Hill and X. Zhang, *Phys. Rev. D* **51**, 3563(1995); Chong-Xing Yue, Yu-Ping Kuang, Xue-Lei Wang and Wei-Bin Li, *Phys. Rev. D* **62**, 055005(2000).
- [21] Xue Lei Wang, Wen Na Xu, Lin Lin Du, *Comn. Theor. Phys.* **41**, 737(2004).
- [22] For reviews on the MSSM, see: P. Fayet and S. Ferrara, *Phys. Rep.* **32**, 249(1977); H. P. Nilles, *Phys. Rep.* **110**, 1(1984); R. Barbieri, *Riv. Nuovo Cim.* **11N4**, 1(1988); J. Bagger, *Lectures at TASI-95*, hep-ph/**9604232**.
- [23] P. M. Ferreira, L. Lavoura, M. N. Rebelo, M. Sher and J. P. Silva, *arXiv:* **1106.0034** [hep-ph].